



Published in final edited form as:

*Sci Signal*. ; 10(478): . doi:10.1126/scisignal.aah5417.

## Membrane depolarization activates BK channels through ROCK-mediated $\beta 1$ subunit surface trafficking to limit vasoconstriction

M. Dennis Leo<sup>1</sup>, Xue Zhai<sup>1</sup>, Padmapriya Muralidharan<sup>1</sup>, Korah P. Kuruvilla<sup>1</sup>, Simon Bulley<sup>1</sup>, Frederick A. Boop<sup>2</sup>, and Jonathan H. Jaggar<sup>1,\*</sup>

<sup>1</sup>Department of Physiology, University of Tennessee Health Science Center, Memphis, TN 38163, USA

<sup>2</sup>Department of Neurosurgery, University of Tennessee Health Science Center, Memphis, TN 38163, USA

### Abstract

Membrane depolarization of smooth muscle cells (myocytes) in the small arteries that regulate regional organ blood flow leads to vasoconstriction. Membrane depolarization also activates large-conductance calcium ( $\text{Ca}^{2+}$ )-activated potassium (BK) channels, which limits  $\text{Ca}^{2+}$  channel activity that promotes vasoconstriction, thus leading to vasodilation. We showed that in human and rat arterial myocytes, membrane depolarization rapidly increased the cell surface abundance of auxiliary BK  $\beta 1$  subunits but not that of the pore-forming BK $\alpha$  channels. Membrane depolarization stimulated voltage-dependent  $\text{Ca}^{2+}$  channels, leading to  $\text{Ca}^{2+}$  influx and the activation of Rho kinase (ROCK) 1 and 2. ROCK1/2-mediated activation of Rab11A promoted the delivery of  $\beta 1$  subunits to the plasma membrane by Rab11A-positive recycling endosomes. These additional  $\beta 1$  subunits associated with BK $\alpha$  channels already at the plasma membrane, leading to an increase in apparent  $\text{Ca}^{2+}$  sensitivity and activation of the channels in pressurized arterial myocytes and vasodilation. Thus, membrane depolarization activates BK channels through stimulation of ROCK- and Rab11A-dependent trafficking of  $\beta 1$  subunits to the surface of arterial myocytes.

\*Corresponding author: jjaggar@uthsc.edu.

#### SUPPLEMENTARY MATERIALS

[www.sciencesignaling.org/cgi/content/full/10/478/eaah5417/DC1](http://www.sciencesignaling.org/cgi/content/full/10/478/eaah5417/DC1)

Fig. S1. Effect of different antagonists on depolarization- and SNP-induced changes in the surface abundance of BK $\alpha$  and  $\beta 1$  protein.

Fig. S2. Depolarization-induced surface trafficking of  $\beta 1$  subunits in human cerebral arteries.

Fig. S3. Overexpression of  $\beta 1$  subunits in HEK293 cells and colocalization analysis of BK $\alpha$ - $\beta 1$  FRET with WGA.

Fig. S4. Effect of Rab11A shRNA or Rab11A dominant-negative mutant on Rab11A abundance and surface BK $\alpha$  protein.

Fig. S5. Regulation of surface BK $\alpha$  protein by antagonists and Cav1.2 and BK $\alpha$  proteins by Cav1.2 siRNA.

Fig. S6. Effect of ROCK 1 or ROCK2 knockdown and HA1100 on respective protein abundance.

Fig. S7. Rab11A knockdown does not alter vasoconstriction by membrane depolarization or myogenic tone.

**Author contributions:** M.D.L., X.Z., P.M., K.P.K., and S.B. performed the experiments and analyzed the data. F.A.B. contributed human samples for the experiments. M.D.L. compiled the data. M.D.L. and J.H.J. wrote the manuscript. All authors approved the final version of the manuscript.

**Competing interests:** The authors declare that they have no competing interests.

## INTRODUCTION

Membrane potential regulates physiological functions in virtually all cell types, including neurons, endocrine cells, and smooth muscle cells (myocytes) of resistance-size arteries that control regional organ blood flow and systemic blood pressure (1). Membrane depolarization in small arteries leads to the activation of myocyte voltage-dependent calcium ( $\text{Ca}^{2+}$ ) ( $\text{Ca}_V1.2$ ) channels, leading to an increase in intracellular  $\text{Ca}^{2+}$  concentration and vasoconstriction. In contrast, membrane hyperpolarization reduces voltage-dependent  $\text{Ca}^{2+}$  channel activity in arterial myocytes, leading to vasodilation. Investigating the physiological processes that control membrane potential is essential to better understand the mechanisms that regulate vascular contractility.

Large-conductance  $\text{Ca}^{2+}$ -activated potassium (BK) channels are found in many different cell types, including arterial myocytes (2). Membrane potential is a key regulator of functional BK channel activity, although mechanisms involved in native cell types are poorly understood (3). Depolarization-induced BK channel activation attenuates voltage-dependent  $\text{Ca}^{2+}$  channel activity in arterial myocytes, limiting vasoconstriction (4, 5). BK channels are tetramers of pore-forming  $\alpha$  ( $\text{BK}\alpha$ ) subunits that can couple to auxiliary  $\beta$  subunits, which comprise a family of four isoforms ( $\beta1$ - $\beta4$ ) (2, 6).  $\beta$ -subunit isoforms are distributed in a tissue-specific manner and can regulate the apparent  $\text{Ca}^{2+}$  sensitivity and gating properties of BK channels to customize cellular functionality (7). Both  $\text{BK}\alpha$  and  $\beta1$  subunits are present in arterial myocytes, and  $\beta1$  subunits increase the apparent  $\text{Ca}^{2+}$  sensitivity of BK channels (8).  $\beta1$  subunits are essential for BK channels to control arterial myocyte contractility and systemic blood pressure (7, 8). Cardiovascular diseases, including atherosclerosis, stroke, and hypertension, are associated with pathological alterations in BK channel  $\beta1$  subunit abundance and function (9). Whether membrane potential controls BK channel activity by modulating interactions between  $\text{BK}\alpha$  and  $\beta1$  subunits is poorly understood, particularly in native cell types.

Membrane current ( $I$ ) generated by a population of ion channels, including BK channels, is the product of the number of channels ( $N$ ), open probability ( $P_o$ ), and single-channel current ( $i$ ). Membrane de-polarization and a rise in intracellular  $\text{Ca}^{2+}$  concentration increase the open probability of BK channels, but whether these activators control the number of plasma membrane BK channel subunits in arterial myocytes and other cell types to modulate cellular functions is unclear (3). In resting arterial myocytes,  $\text{BK}\alpha$  subunits are essentially plasma membrane-localized proteins that are surface-trafficked by Rab4A-positive early endosomes (10). In contrast, only a small proportion of total  $\beta1$  subunit protein is located at the plasma membrane, with much of the intracellular  $\beta1$  protein stored within mobile Rab11A-positive recycling endosomes (11). Here, we tested the hypothesis that membrane potential and the intracellular  $\text{Ca}^{2+}$  concentration control the surface abundance of  $\text{BK}\alpha$  and  $\beta1$  subunits to regulate channel activity and contractility in arterial myocytes.

We showed that membrane depolarization, through the stimulation of voltage-dependent  $\text{Ca}^{2+}$  channels and  $\text{Ca}^{2+}$  influx, activated Rho kinase (ROCK) 1 and 2, which phosphorylated Rab11A, leading to the rapid delivery of intracellular  $\beta1$  subunits to the plasma membrane in arterial myocytes. These  $\beta1$  subunits increased the apparent  $\text{Ca}^{2+}$

sensitivity of plasma membrane–resident BK channels, resulting in an increase in BK channel open probability and vasodilation. Thus, we describe a mechanism by which membrane potential regulates functional BK channel activity through the modulation of ROCK-dependent trafficking of  $\beta 1$  subunits to the surface.

## RESULTS

### Membrane depolarization increases the surface abundance of BK channel $\beta 1$ subunits in arterial myocytes

Cellular distribution of BK $\alpha$  and  $\beta 1$  subunits was measured in myocytes of intact resistance-size (diameter of  $\sim 200$   $\mu\text{m}$ ) cerebral arteries using surface biotinylation. Regulation by membrane potential was studied by increasing the extracellular  $\text{K}^+$  concentration in the bath solution from 6 to either 30 or 60 mM, which depolarizes arteries from  $\sim -60$  to  $-40$  or  $-20$  mV, respectively (12). In rat cerebral arteries maintained in physiological saline solution (PSS) containing 6 mM extracellular  $\text{K}^+$ ,  $\sim 95.5\%$  of total BK $\alpha$  and  $\sim 7.7\%$  of total  $\beta 1$  subunits were plasma membrane–localized (Fig. 1, A and B, and fig. S1, A to D). Increasing bath extracellular  $\text{K}^+$  to 30 or 60 mM stimulated a  $\sim 2.7$ - or  $\sim 3.2$ -fold increase in surface  $\beta 1$  protein, respectively (Fig. 1, A and B). Depolarization increased surface  $\beta 1$  protein within 1 min, the shortest time point measured (Fig. 1, A and B). In contrast, membrane depolarization did not alter surface BK $\alpha$  protein (Fig. 1A and fig. S1, C and D). Arterial repolarization, produced by returning depolarized arteries to a bath solution containing 6 mM extracellular  $\text{K}^+$ , reversed the depolarization-induced increase in surface  $\beta 1$  protein by  $\sim 75\%$  in 1 min and completely in 10 min (fig. S1, E and F). Similar data were obtained in human cerebral arteries, where depolarization (30 mM  $\text{K}^+$ ) increased surface  $\beta 1$   $\sim 2.4$ -fold but did not alter surface BK $\alpha$  (fig. S2, A and B). Brefeldin A, an endoplasmic reticulum–to–Golgi trafficking inhibitor, blocked depolarization-induced  $\beta 1$  subunit surface trafficking but did not alter surface BK $\alpha$  (Fig. 1, A and B, and fig. S1, C and D).  $\beta 1$  subunit antibody specificity was confirmed with lysates from recombinant  $\beta 1$ -transfected human embryonic kidney (HEK) 293 cells. The  $\beta 1$  antibody did not identify a protein in lysate from mock-transfected HEK293 cells but detected a band of  $\sim 34$  kDa in cells expressing recombinant  $\beta 1$ , which was similar in molecular mass to that of arterial  $\beta 1$  protein (fig. S3A). These data indicate that membrane depolarization stimulates intracellular  $\beta 1$  subunits to traffic to the plasma membrane in rat and human cerebral artery myocytes.

Immunofluorescence Förster resonance energy transfer (FRET) imaging was used to examine the regulation of BK $\alpha$  and  $\beta 1$  subunit spatial proximity by membrane depolarization in isolated arterial myocytes. The Förster coefficient for the Alexa 488–Alexa 546 FRET pair used for these experiments is  $\sim 6.3$  nm. Membrane depolarization, produced by increasing extracellular  $\text{K}^+$  concentration in the bath solution from 6 to 60 mM, contracted arterial myocytes and increased mean normalized FRET between BK $\alpha$ - and  $\beta 1$ -bound secondary antibodies  $\sim 3.4$ -fold (Fig. 1, C and D). Returning depolarized (60 mM  $\text{K}^+$ ) myocytes to a bath solution containing 6 mM  $\text{K}^+$  (10 min) reversed the increase in normalized FRET (Fig. 1, C and D). Brefeldin A abolished the depolarization-induced increase in BK $\alpha$ - $\beta 1$  normalized FRET (Fig. 1, C and D). In depolarized cells (30 mM  $\text{K}^+$ ), colocalization of FRET with wheat germ agglutinin (WGA), a plasma membrane marker,

produced a coefficient of  $\sim 93.3 \pm 1.3\%$ , indicating that most of the BK $\alpha$ - $\beta 1$  signal occurs at the surface (fig. S3B). These data suggest that membrane depolarization stimulates surface trafficking of  $\beta 1$  subunits, which then associate with plasma membrane-resident BK $\alpha$  channels in arterial myocytes.

By acting through soluble guanylyl cyclase (sGC) and guanosine 3',5'-monophosphate-dependent protein kinase (PKG), nitric oxide (NO) stimulates the surface trafficking of  $\beta 1$  subunits that reside within Rab11A-positive recycling endosomes in arterial myocytes (11). Here, we investigated whether membrane depolarization and NO mobilize the same, or different,  $\beta 1$  protein pools. The NO donor sodium nitroprusside (SNP) increased surface  $\beta 1$  protein  $\sim 2.5$ -fold in arteries in a 6 mM K $^{+}$ -containing PSS and  $\sim 3.6$ -fold in arteries in 30 mM K $^{+}$  and did not further increase surface  $\beta 1$  protein in arteries in 60 mM K $^{+}$  when compared to 30 mM K $^{+}$  (Fig. 1B and fig. S1B). The sGC inhibitor 1*H*-[1,2,4]oxadiazolo[4,3-*a*]quinoxalin-1-one (ODQ) and the protein kinase G inhibitor DT-2 blocked the surface trafficking of  $\beta 1$  subunits induced by SNP but not by depolarization (fig. S1, A and B). SNP, ODQ, and DT-2 did not alter surface BK $\alpha$  protein (fig. S1, C and D). These data indicate that membrane depolarization and NO activate different signaling pathways to stimulate an increase in the surface abundance of  $\beta 1$  subunits.

To investigate the source of  $\beta 1$  subunits mobilized by membrane depolarization, we used RNA interference. Short hairpin RNAs (shRNAs) targeting Rab11A reduced Rab11A protein to  $\sim 48\%$  of scrambled shRNA controls in arteries (fig. S4, A and C). Rab11A knockdown abolished the depolarization-induced increase in  $\beta 1$  surface abundance in arteries and the increase in normalized FRET between BK $\alpha$  and  $\beta 1$  subunits in isolated myocytes (Fig. 2, A to D). A Rab11A dominant-negative (Rab11AS25N) mutant also blocked the depolarization-induced increase in the surface abundance of  $\beta 1$  subunits (Fig. 2, E and F, and fig. S4, B and C). Rab11A knockdown or the Rab11A dominant-negative mutant did not alter surface BK $\alpha$  protein (fig. S4D). These data indicate that membrane depolarization and NO activate distinct intracellular signaling pathways to mobilize the same intracellular pool of  $\beta 1$  subunits that reside within Rab11A-positive recycling endosomes.

### Voltage-dependent Ca $^{2+}$ channel activity controls $\beta 1$ subunit surface abundance

Next, we investigated signaling pathways by which membrane potential controls the surface abundance of  $\beta 1$  subunits. Membrane depolarization stimulates voltage-dependent Ca $^{2+}$  channels, leading to an increase in the intracellular Ca $^{2+}$  concentration in arterial myocytes (1, 13). Ca $^{2+}$ -free PSS or the Ca $_v$ 1.2 channel blocker nimodipine inhibited depolarization-induced  $\beta 1$  subunit trafficking (Fig. 3, A and B). Ca $_v$ 1.2 small interfering RNA (siRNA) decreased Ca $_v$ 1.2 protein by  $\sim 60\%$  and reduced depolarization-induced  $\beta 1$  subunit trafficking by  $\sim 75\%$  of scrambled siRNA controls (fig. S5, B and C, and Fig. 3, C and D). These findings confirmed the role of Ca $^{2+}$  influx in mediating the  $\beta 1$  surface trafficking through Ca $_v$ 1.2. Membrane depolarization stimulates local intracellular Ca $^{2+}$  transients termed Ca $^{2+}$  sparks, which activate BK channels in arterial myocytes (4). Ryanodine, a ryanodine-sensitive Ca $^{2+}$ -release channel (RyR) blocker that inhibits Ca $^{2+}$  sparks, did not alter depolarization-induced  $\beta 1$  trafficking (Fig. 3B). Ca $_v$ 1.2 knockdown, nimodipine, or ryanodine did not alter BK $\alpha$  surface protein (Fig. 3A and fig. S5, A and D). These data

indicate that membrane potential control of voltage-dependent  $\text{Ca}^{2+}$  channel activity and  $\text{Ca}^{2+}$  influx regulates  $\beta 1$  subunit surface abundance.

### Membrane depolarization stimulates ROCK-dependent phosphorylation of Rab11A to activate $\beta 1$ subunit trafficking

An increase in intracellular  $\text{Ca}^{2+}$  concentration can activate several kinases, including ROCK,  $\text{Ca}^{2+}$ /calmodulin-dependent protein kinase II (CaMKII), phosphoinositide 3-kinase (PI3K), and protein kinase C (PKC) in arterial myocytes (14–17). The ROCK inhibitor HA1100 attenuated depolarization-induced  $\beta 1$  surface trafficking (Fig. 3, A and B). In contrast, the CaMKII inhibitor KN93, the PI3K inhibitor LY294002, or the PKC inhibitor bisindolylmaleimide (BIM II) did not alter depolarization-induced  $\beta 1$  trafficking (Fig. 3B).

Both ROCK1 and ROCK2 are present in arterial myocytes (18). To examine ROCK isoforms involved, we transfected arteries with siRNA targeting either ROCK1 or ROCK2. ROCK1 siRNA reduced ROCK1 protein to ~50% of scrambled siRNA controls, whereas ROCK2 siRNA reduced ROCK2 protein to ~47% of controls (fig. S6, A and B). Each siRNA did not alter the amount of the other ROCK isoform, indicating selectivity (fig. S6, A and B). ROCK1- and ROCK2-specific knockdown each reduced depolarization-induced  $\beta 1$  trafficking by ~91 and ~70%, respectively, of scrambled siRNA controls (Fig. 3, E and F). In contrast, ROCK1 or ROCK2 knockdown did not alter surface  $\text{BK}\alpha$  (Fig. 3, E and F, and fig. S6C). These experiments suggest that depolarization activates ROCK1 and ROCK2, which stimulate  $\beta 1$  subunit anterograde trafficking, leading to an increase in  $\beta 1$  surface abundance in arterial myocytes.

Next, we tested the hypothesis that activated ROCK phosphorylated Rab11A. Membrane depolarization increased guanosine 5'-triphosphate-bound active Rab11 in arteries, an effect that was inhibited by HA1100 (Fig. 4, A and B). In contrast, depolarization alone or in the presence of HA1100 did not alter Rab11A,  $\beta 1$ , or  $\text{BK}\alpha$  total protein (Fig. 4A and fig. S6D). Together, these data indicate that membrane depolarization stimulates voltage-dependent  $\text{Ca}^{2+}$  channels, leading to  $\text{Ca}^{2+}$  influx and the activation of ROCK1/2, which phosphorylates Rab11A, thereby promoting the surface trafficking of Rab11A-positive recycling endosomes that deliver  $\beta 1$  subunits to the plasma membrane.

### Depolarization-induced $\beta 1$ subunit trafficking increases the apparent $\text{Ca}^{2+}$ sensitivity of BK channels in arterial myocytes

$\beta 1$  subunits increase the apparent  $\text{Ca}^{2+}$  sensitivity of BK channels, leading to channel activation (7, 19). To study the regulation of BK channel activity by depolarization-induced  $\beta 1$  subunit trafficking, we performed patch-clamp electrophysiology. Inside-out patches were pulled from myocytes that had been exposed to a bath solution containing either 6 mM  $\text{K}^+$  (control), 30 mM  $\text{K}^+$ , or 30 mM  $\text{K}^+$  plus HA1100. After patch excision, bath solutions were then changed so that the apparent  $\text{Ca}^{2+}$  sensitivity of BK channels was measured in membrane patches under identical conditions, in symmetrical  $\text{K}^+$  at  $-40$  mV, a physiological membrane voltage. In control myocytes, the mean apparent dissociation constant ( $K_d$ ) for  $\text{Ca}^{2+}$  of BK channels was ~34  $\mu\text{M}$ , with a maximum open probability of  $\sim 0.80 \pm 0.02$  (Fig. 4, C and D). In patches pulled from myocytes placed in 30 mM  $\text{K}^+$  bath solution, the mean

$K_d$  for  $Ca^{2+}$  of BK channels was  $\sim 9 \mu M$  or 3.8-fold higher, without an alteration in maximal open probability ( $0.80 \pm 0.03$ ; Fig. 4, C and D). HA1100 blocked the 30 mM  $K^+$  bath solution from increasing the  $Ca^{2+}$  sensitivity of BK channels but did not change maximal open probability ( $0.08 \pm 0.03$ ; Fig. 4, C and D). These data indicate that membrane depolarization activates ROCK to increase BK channel apparent  $Ca^{2+}$  sensitivity in arterial myocytes.

Lithocholate, a specific activator of  $\beta 1$  subunit-containing BK channels, was used to study regulation of BK channels. We examined whether lithocholate would be a more effective activator of BK channels that contain additional depolarization-trafficked  $\beta 1$  subunits. Lithocholate increased BK channel mean open probability in inside-out patches pulled from both control (6 mM  $K^+$ ) and 30 mM  $K^+$ -treated myocytes (Fig. 4, C and E). Moreover, lithocholate increased mean open probability 2.74  $\pm$  0.02-fold more in 30 mM  $K^+$ -treated myocytes than in 6 mM  $K^+$ -treated myocytes, consistent with the hypothesis being tested (Fig. 4, C and E). HA1100 attenuated the depolarization-induced increase in BK channel open probability (Fig. 4, C and E). These data indicate that depolarization-stimulated  $\beta 1$  subunit surface trafficking increases BK channel  $Ca^{2+}$  sensitivity and activation by a  $\beta 1$  ligand and that, overall, depolarization increases the amount of  $\beta 1$  subunits associated with BK channels.

### **Intravascular pressure stimulates BK channels through Rab11A activation in arterial myocytes**

Intravascular pressure stimulates BK channels in arterial myocytes (20). We tested whether Rab11A-mediated  $\beta 1$  subunit trafficking contributed to intravascular pressure-induced BK channel activation in arterial myocytes. ROCK could not be manipulated for these contractile measurements because this kinase contributes to myocyte contraction through multiple mechanisms, including phosphorylation of myosin phosphatase, myosin light chain (MLC) kinase, and CPI-17 (21). In pressurized, myogenic (60 mmHg) control arteries transfected with scrambled siRNA, the BK channel activator NS1619 stimulated a mean vasodilation of  $\sim 34.7 \mu m$ , and the specific BK channel inhibitor, iberiotoxin, produced a mean constriction of  $\sim 25.5 \mu m$  (Fig. 5, A and B). Lithocholate dilated control arteries by  $\sim 9.7 \mu m$  (Fig. 5, A and C). Rab11A knockdown reduced mean NS1619- and lithocholate-induced vaso-dilation and iberiotoxin-induced vasoconstriction to  $\sim 17.6$ , 4.6, and 13  $\mu m$ , respectively, which are  $\sim 49.3$ ,  $\sim 47.0$ , and  $\sim 51.0\%$  of those in scrambled controls (Fig. 5, A to C). Rab11A knockdown did not alter vasoconstriction stimulated by membrane depolarization or myogenic tone (fig. S7, A and B). These data demonstrate that intravascular pressure stimulates BK channels through Rab11A-induced  $\beta 1$  subunit trafficking in arterial myocytes.

## **DISCUSSION**

Intravascular pressure-induced membrane depolarization activates BK channels in arterial myocytes (4, 5). Here, we described a mechanism by which intravascular pressure and membrane potential controlled BK channel activity by modulating the plasma membrane abundance of auxiliary  $\beta 1$  subunits in arterial myocytes. Our data indicated that membrane



depolarization stimulated voltage-dependent  $\text{Ca}^{2+}$  channels, leading to  $\text{Ca}^{2+}$  influx and ROCK1 and ROCK2 activation. We showed that ROCK phosphorylated Rab11A, stimulating anterograde trafficking of Rab11A-positive recycling endosomes, which delivered intracellular  $\beta 1$  subunits to the plasma membrane. These  $\beta 1$  subunits associated with plasma membrane-resident BK channels, increasing their apparent  $\text{Ca}^{2+}$  sensitivity and leading to channel activation and vasodilation. Thus, we showed that membrane depolarization, through ROCK-dependent stimulation of Rab11A-dependent  $\beta 1$  surface trafficking, activated BK channels in arterial myocytes to modulate arterial contractility.

Physiological intravascular pressures stimulate arterial depolarization between  $\sim -60$  and  $-35$  mV, with the entire contractile range of cerebral arteries occurring between membrane potentials of  $\sim -60$  and  $-25$  mV (4). This depolarization range stimulates voltage-dependent  $\text{Ca}^{2+}$  channels, leading to an increase in “global” intracellular  $\text{Ca}^{2+}$  concentration from  $\sim 100$  to  $350$  nM in arterial myocytes (4). BK channels are sensitive to micromolar intracellular  $\text{Ca}^{2+}$  concentrations, as shown here and elsewhere (11, 22–24). Thus, global intracellular  $\text{Ca}^{2+}$  concentration is inadequate to substantially alter BK channel open probability (4). BK channels in arterial myocytes are activated by  $\text{Ca}^{2+}$  sparks, which are local micromolar  $\text{Ca}^{2+}$  transients that occur due to the release of sarcoplasmic reticulum  $\text{Ca}^{2+}$  through RyR channels (4). A single  $\text{Ca}^{2+}$  spark activates several nearby BK channels, leading to a transient BK current (4). Here, data indicated that membrane depolarization rapidly stimulated anterograde trafficking and plasma membrane insertion of intracellular  $\beta 1$  subunits, which associated with surface  $\text{BK}\alpha$  and increased apparent  $\text{Ca}^{2+}$  sensitivity. We showed that a small proportion of total  $\beta 1$  subunits are present in the plasma membrane of resting ( $\sim -60$  mV) arterial myocytes and that depolarization within a physiological membrane potential range rapidly increased surface  $\beta 1$  protein abundance. Several lines of evidence support a requirement for  $\beta 1$  subunits in depolarization-induced BK channel activation.  $\text{Ca}^{2+}$  spark to BK channel coupling and contractility regulation by BK channels are abolished in  $\beta 1$  subunit knockout mice (8). Analysis of recombinant proteins demonstrates that a BK channel tetramer can contain between one and four  $\beta 1$  subunits and that the  $\alpha/\beta 1$ -tetramer ratio can shift BK channel voltage and  $\text{Ca}^{2+}$  dependence (25–27). Consistent with these findings, BK channel  $\text{Ca}^{2+}$  sensitivity and transient BK current amplitude were both low at resting potentials and increased with physiological membrane depolarization [here and in (24)].  $\beta 1$  subunits increase BK channel apparent  $\text{Ca}^{2+}$  sensitivity in arterial myocytes (6). Our data indicated that membrane depolarization stimulated Rab11A-positive recycling endosomes to deliver  $\beta 1$  subunits to the plasma membrane. The  $\beta 1$  subunit-mediated increase in  $\text{Ca}^{2+}$  sensitivity should enhance BK channel coupling to  $\text{Ca}^{2+}$  sparks, leading to an increase in transient BK currents and vasodilation.

Previous studies of recombinant BK channel proteins have shown that the association of  $\beta 1$  with  $\text{BK}\alpha$  either does not alter the slope of the  $P_0$ - $[\text{Ca}^{2+}]$  curve or can increase the slope (28–30). Whether  $\beta 1$  subunits regulate the slope of the  $P_0$ - $[\text{Ca}^{2+}]$  curve in arterial myocytes was unclear. Data here and in a previous study (11) both demonstrated that depolarization-induced and NO-induced surface trafficking of  $\beta 1$  subunits increased the apparent  $\text{Ca}^{2+}$  sensitivity of BK channels but did not alter the slope of the  $P_0$ - $[\text{Ca}^{2+}]$  curve in arterial myocytes. Several factors may explain different results obtained from investigations of both recombinant and native arterial myocyte BK channels, including splice variants and mutants

studied and the presence or absence of other proteins. Regulatory proteins may also be involved, including auxiliary  $\gamma 1$  subunits, which modify both BK channel modulation by  $\beta 1$  subunits and BK channel properties in arterial myocytes (31, 32).

We showed that depolarization, through a  $\text{Ca}_V1.2$ - and  $\text{Ca}^{2+}$  influx-dependent mechanism, activated ROCK, leading to Rab11A-mediated  $\beta 1$  subunit trafficking in arteries. In contrast, PKC, PI3K, or CaMKII were not involved in depolarization-induced  $\beta 1$  subunit trafficking. A depolarization-induced increase in intracellular  $\text{Ca}^{2+}$  concentration stimulates Rho, leading to ROCK activation in rabbit aortic myocytes (17), providing further support for a  $\text{Ca}^{2+}$ -dependent mechanism. The ROCK pathway regulates multiple cellular functions, including contraction and proliferation, and is associated with cardiovascular diseases (18). Substrates of ROCK include MLC and myosin phosphatase target subunit 1, modulation of which regulates myosin  $\text{Ca}^{2+}$  sensitivity and vascular myocyte contractility (18). Here, knockdown of either ROCK1 or ROCK2 inhibited depolarization-induced  $\beta 1$  trafficking, indicating a requirement for both isoforms. Several reasons may explain why both isoforms are necessary, including that they function in a series signaling cascade. ROCKs homodimerize, suggesting that they may also form a heterodimeric protein that controls  $\beta 1$  trafficking in arterial myocytes (33). ROCK may stimulate recycling endosome trafficking by directly phosphorylating Rab11A or may act upstream by phosphorylating one or more kinases that control Rab11A activity. The Rab11A dominant-negative mutant used here (S25N), which blocked depolarization-induced  $\beta 1$  trafficking, is guanosine diphosphate-bound and inactive. Analysis of the Rab11A amino acid sequence [using an open-source online software, Prediction of PK-Specific Phosphorylation (PPSP) (34)] revealed five potential phosphorylation sites for ROCK, at Thr<sup>32</sup>, Thr<sup>43</sup>, Thr<sup>77</sup>, Thr<sup>98</sup>, and Ser<sup>149</sup>. It was beyond the scope of this study to determine whether ROCK indirectly activated Rab11A or directly phosphorylated Rab11A and which, if any, of these potential phosphorylation sites are involved in  $\beta 1$  trafficking. Future studies should test these hypotheses. In summary, data indicated that membrane depolarization activated  $\text{Ca}_V1.2$  channels, leading to the stimulation of ROCK1 and ROCK2, which activated Rab11A to deliver  $\beta 1$  subunits to the plasma membrane in arterial myocytes.

NO stimulates a rapid increase in the surface abundance of  $\beta 1$  subunits in arterial myocytes, leading to BK channel activation and vasodilation (11). Data here indicated that depolarization and NO mobilized the same intracellular  $\beta 1$  subunit pool but through distinct mechanisms. NO acts through PKG, whereas membrane depolarization functions through  $\text{Ca}_V1.2$  channels and ROCK. NO increases surface  $\beta 1$  protein in nondepolarized arterial myocytes at resting potentials of  $\sim -60$  mV (11), and we showed that NO also stimulated an increase in surface  $\beta 1$  protein at membrane potentials of  $\sim -40$  mV, similar to that in arteries at a physiological intravascular pressure of  $\sim 60$  mmHg (12). In addition to supporting previous findings, these data indicate that at physiological membrane potentials found in pressurized arteries, NO increases surface  $\beta 1$  to stimulate vasodilation (11).

Biochemical and functional data demonstrate that  $\beta 1$  surface abundance in arterial myocytes is controlled by both Rab11A-dependent and Rab11A-independent mechanisms (11). Here, Rab11A knockdown blocked the depolarization-induced increase in both surface  $\beta 1$  subunits and BK channel apparent  $\text{Ca}^{2+}$  sensitivity but did not abolish diameter responses to BK



channel modulators in pressurized arteries. Because  $\text{Ca}^{2+}$  spark inhibition in myocytes abolishes vasoregulation by BK channels (35), our data suggest coupling of BK channels to  $\text{Ca}^{2+}$  sparks when depolarization-induced, Rab11A-dependent  $\beta 1$  subunit trafficking is blocked. We showed that a population of surface  $\beta 1$  subunits existed in close proximity to plasma membrane BK $\alpha$  proteins that were not modulated by Rab11A knockdown or Rab11A mutants or by NO, brefeldin A, nocodazole, nimodipine, or HA1100 (11). The trafficking mechanism controlling the surface abundance of these “basal”  $\beta 1$  subunits is unclear but appears to be voltage-, Rab11A-, Rab4A-, and sGC/PKG-independent [data here and in (10, 11)]. These surface  $\beta 1$  subunits may generate a baseline amount of BK channel coupling to  $\text{Ca}^{2+}$  sparks in myocytes.

In summary, we showed that membrane depolarization stimulated  $\text{Ca}_v1.2$  channels, leading to  $\text{Ca}^{2+}$  influx and the activation of ROCK, which phosphorylated Rab11A, promoting surface trafficking of Rab11A-positive recycling endosomes that delivered  $\beta 1$  subunits to the plasma membrane. The increase in surface  $\beta 1$  enhanced BK channel apparent  $\text{Ca}^{2+}$  sensitivity and functional BK channel activity in pressurized arteries.

## MATERIALS AND METHODS

### Chemicals

SNP, DT-2, ODQ, brefeldin A, ryanodine, KN93, LY294002, and NS1619 were purchased from Sigma-Aldrich and were used at a final concentration of 10  $\mu\text{M}$ . Gadolinium chloride was from Sigma-Aldrich and used at a final concentration of 100  $\mu\text{M}$ . Nimodipine (Sigma-Aldrich) was used at 1  $\mu\text{M}$ . HA1100 and BIM II were from Cayman Chemical and were used at a final concentration of 10  $\mu\text{M}$ . Iberiotoxin (Sigma-Aldrich) was used at a concentration of 100 nM. Lithocholate (Steraloids Inc.) was used at a final concentration of 50  $\mu\text{M}$  and was dissolved as previously described (36).

### Tissue preparation and smooth muscle cell isolation

All animal protocols were reviewed and approved by the Animal Care and Use Committee at the University of Tennessee Health Science Center. Sprague-Dawley rats (male, 7 to 8 weeks) were used for all experiments and were randomly picked from a lot. Euthanasia was performed by intraperitoneal injection of sodium pentobarbital (150 mg/kg). The brain was removed, and cerebral arteries were dissected, cleaned, and placed in chilled oxygenated (21%  $\text{O}_2$ , 5%  $\text{CO}_2$ , and 74%  $\text{N}_2$ ) PSS of the following composition: 119 mM NaCl, 4.7 mM KCl, 24 mM  $\text{NaHCO}_3$ , 1.2 mM  $\text{KH}_2\text{PO}_4$ , 1.6 mM  $\text{CaCl}_2$ , 1.2 mM  $\text{MgSO}_4$ , and 11 mM glucose (pH 7.4). Myocytes were enzymatically dissociated from isolated arteries, as previously described (37). All experiments involving dissociated myocytes were completed on the same day of isolation. Human brain samples were obtained after Institutional Review Board approval and written informed consent from patients and in accordance with the guidelines of the Declaration of Helsinki. The samples obtained were from a 13- and 17-year-old males and a 25-year-old female patient who underwent a lobectomy and were reported to have no history of hypertension or stroke.

### Transfection of intact cerebral arteries

Rab11A short hairpin vector (shV) and scrambled shV were purchased from OriGene Technologies Inc. Rat rab11A cDNA was obtained from a clone library (GenScript USA Inc.). A dominant-negative mutant of Rab11A with serine-to-asparagine mutation (Rab11AS25N) was generated and subcloned into pcDNA3.1(+) (Life Technologies). Ca<sub>v</sub>1.2, ROCK1, ROCK2, and scrambled siRNAs were obtained from Life Technologies. Cerebral arteries were transfected using a CUY21Vivo-SQ electroporator (BEX Co. Ltd.). Cerebral arteries were placed in an electroporation chamber in Ca<sup>2+</sup>-free phosphate-buffered saline containing the vector or siRNA. Tandem pulse electroporation was applied. Arteries were then removed and kept in Ca<sup>2+</sup>-free phosphate-buffered saline for 10 min, after which they were placed in serum-free Dulbecco's Modified Eagle Medium/Nutrient Mixture F-12 (DMEM/ F-12) supplemented with 1% penicillin-streptomycin (Sigma-Aldrich) for 3 days under standard conditions (21% O<sub>2</sub>, 5% CO<sub>2</sub>, and 74% N<sub>2</sub>; 37°C). At the end of the incubation period, the arteries were washed once in chilled PSS solution and used for surface biotinylation or immunofluorescence resonance energy transfer (immunoFRET) experiments.

### Surface biotinylation

Cellular distribution of BK $\alpha$  and  $\beta$ 1 proteins in intact cerebral arteries was determined using surface biotinylation at room temperature, as previously described (38). Arteries were incubated for 1 hour in a 1 mg/ml mixture each of EZ-Link Sulfo-NHS-LC-LC-Biotin and EZ-Link Maleimide-PEG2-Biotin reagents (Pierce) in Hepes-buffered PSS solution containing 134 mM NaCl, 6 mM KCl, 10 mM Hepes, 2 mM CaCl<sub>2</sub>, 1 mM MgCl<sub>2</sub>, and 10 mM glucose (pH 7.4 with NaOH) at room temperature, after which arteries were exposed to test conditions at room temperature. To measure reversal of depolarization-induced  $\beta$ 1 subunit trafficking, arteries were exposed to 60 mM K<sup>+</sup>-containing PSS for 10 min, transferred to 6 mM K<sup>+</sup> PSS for either 1 or 10 min at room temperature, and then biotinylated in chilled solution at 4°C for 1 hour. The reaction was quenched using 100 mM glycine in phosphate-buffered saline followed by washing in phosphate-buffered saline. Biotinylated arteries were homogenized in a lysis buffer consisting of 50 mM Tris-HCl, 150 mM NaCl, 5 mM EDTA, 1% Triton X-100, and 0.1% SDS. Total protein was estimated, as previously described (39), to allow normalization for pull-down. Biotinylated proteins were pulled down using monomeric avidin beads (Pierce). The nonbiotinylated supernatant contained the intracellular protein fraction. Biotinylated plasma membrane proteins that were bound to avidin beads were eluted by boiling in Laemmli buffer (with 5%  $\beta$ -mercaptoethanol). Cellular distribution of proteins was analyzed by Western blotting and calculated as a percentage of total protein.

### Western blot analysis

A standard 7.5% SDS-polyacrylamide gel was used for separation of proteins, which were then transferred onto nitrocellulose membranes. Blots were physically cut between ~50 and 75 kDa to probe the same protein samples for BK $\alpha$  and  $\beta$ 1 without stripping. Membranes were then incubated with a mouse monoclonal antibody recognizing BK $\alpha$  (1:500 dilution; NeuroMab, University of California, Davis), a rabbit polyclonal antibody recognizing BK $\beta$ 1

(1:500; Abcam), a mouse monoclonal antibody recognizing rab11A (1:500; Abcam), a mouse monoclonal antibody recognizing Cav1.2 (1:100; NeuroMab), a rabbit monoclonal antibody recognizing ROCK1 (1:500; Cell Signaling), a rabbit polyclonal antibody recognizing ROCK2 (1:500; Cell Signaling), or a mouse monoclonal antibody recognizing active rab11 (1:500; NewEast Biosciences) antibodies overnight at 4°C in tris-buffered saline (TBS) with 0.1% Tween 20 and 5% nonfat dry milk. Proteins were visualized using appropriate horseradish peroxidase-conjugated secondary antibodies (Pierce) and a chemiluminescent detection kit (Pierce). Band intensity was quantified by digital densitometry using Quantity One software (Bio-Rad).

### Confocal imaging and immunoFRET

ImmunoFRET was performed similarly, as previously described (40). Myocytes were exposed to 60 mM K<sup>+</sup>-containing PSS for 10 min and either fixed or then exposed to 6 mM K<sup>+</sup>-containing PSS for 10 min to measure reversal and then fixed. Myocytes were fixed with paraformaldehyde and permeabilized with 0.1% Triton X-100 for 2 min at room temperature. One hour after incubation in phosphate-buffered saline containing 5% bovine serum albumin, myocytes were treated overnight at 4°C with a mouse monoclonal antibody recognizing BK $\alpha$  (NeuroMab, University of California, Davis) and a rabbit polyclonal antibody recognizing BK $\beta$ 1 (Abcam). Antibodies were used at a dilution of 1:100 each in phosphate-buffered saline containing 5% bovine serum albumin. After washes in phosphate-buffered saline, cells were incubated at 37°C for 1 hour with secondary antibodies: Alexa 546-conjugated or Alexa 488-conjugated (1:100 dilution; Life Technologies). Coverslips were then washed and mounted on glass slides. For colocalization experiments, Alexa 633-conjugated WGA was first incubated with fixed cells for 10 min, after which myocytes were processed, as described above. Fluorescence images were acquired using a Zeiss LSM Pascal confocal microscope. Alexa 488 and Alexa 546 were excited at 488 and 543 nm, and emissions were collected at 505 to 530 and >560 nm, respectively. A z-resolution of ~1  $\mu$ m was used. For FRET analysis, the following background values were determined: the donor and acceptor signal in the absence of FRET, cross-talk of the donor and acceptor signals into the FRET channel, and the FRET signal from the donor and acceptor channels, respectively. After background subtraction, normalized FRET was calculated on a pixel-by-pixel basis for the entire image using the method of Xia and Liu (41) and Zeiss LSM FRET Macro tool version 2.5. FRET pixel colocalization with WGA was calculated using the Mander's colocalization plugin for ImageJ (version 1.51h, National Institutes of Health). The RG2B plugin for ImageJ was used to colocalize FRET and WGA pixels in images.

### Patch-clamp electrophysiology

Single BK channel currents were recorded in isolated myocytes using the inside-out patch clamp configuration (Axopatch 200B and Clampex 8.2, MDS Analytical Technologies). Myocytes were allowed to settle, and inside-out patches were pulled in 6 mM K<sup>+</sup>-containing or 30 mM K<sup>+</sup>-containing Hepes-buffered PSS. The composition of the pipette and bath solution during patch recordings was 130 mM KCl, 10 mM Hepes, 1 mM MgCl<sub>2</sub>, 5 mM EGTA, and 1.6 mM HEDTA (pH 7.2) with KOH. Free Ca<sup>2+</sup> concentration was adjusted to between 1 and 300  $\mu$ M by adding CaCl<sub>2</sub>, and free Mg<sup>2+</sup> was maintained at 1 mM using MgCl<sub>2</sub>. Free Ca<sup>2+</sup> concentration in solutions was measured using Ca<sup>2+</sup>-sensitive (no.

476041, Corning) and reference (no. 476370, Corning) electrodes. Control myocytes did not receive any treatment. In some experiments, HA1100 (10  $\mu\text{M}$ ) was applied for 30 min before 30 mM  $\text{K}^+$ -containing PSS treatment. Inside-out patch experiments were performed at a membrane voltage of  $-40$  mV. Currents were filtered at 1 kHz and digitized at 5 kHz. Analysis was performed offline using Clampfit 9.2 (MDS Analytical Technologies). Data from the  $\text{Ca}^{2+}$  sensitivity experiments were fit with an unconstrained single Boltzmann function where the midpoint was between the minimal and maximal amplitudes of each fit.

### Pressurized artery myography

Endothelium-denuded arterial segments of 1 to 2 mm in length were cannulated in a perfusion chamber (Living Systems Instrumentation) maintained at  $37^\circ\text{C}$  and continuously perfused with PSS (pH 7.4) gassed with 21%  $\text{O}_2$ , 5%  $\text{CO}_2$ , and 74%  $\text{N}_2$ . Arterial diameter was measured at 1 Hz using a charge-coupled device camera attached to a Nikon TS100-F microscope and the automatic edge-detection function of IonWizard software (IonOptix). Luminal flow was absent during experiments. Myogenic tone (%) was calculated as follows:  $100 \times (1 - D_{\text{active}}/D_{\text{passive}})$ , where  $D_{\text{active}}$  is the active arterial diameter and  $D_{\text{passive}}$  is the diameter determined in the presence of  $\text{Ca}^{2+}$ -free PSS supplemented with 5 mM EGTA.

### Statistical analysis

GraphPad Prism version 4.0 and Origin version 6.0 were used for statistical analyses. Values are presented as means  $\pm$  SE. Student's  $t$  test was used for comparing paired and unpaired data from two populations. For multiple-group comparisons, analysis of variance (ANOVA) with Student-Newman-Keuls post hoc test was used.  $P < 0.05$  was considered significant. Power analysis was performed to verify that the sample size gave a value of  $>0.8$  if  $P$  was  $>0.05$ .

### Supplementary Material

Refer to Web version on PubMed Central for supplementary material.

### Acknowledgments

We thank M. Kocak (associate professor, Department of Biostatistics, University of Tennessee Health Science Center) for reviewing the statistical methods used in this manuscript.

**Funding:** This study was supported by NIH/NHLBI (National Heart, Lung, and Blood Institute) grants to J.H.J. and American Heart Association grants to M.D.L. and S.B.

### REFERENCES AND NOTES

1. Nelson MT, Patlak JB, Worley JF, Standen NB. Calcium channels, potassium channels, and voltage dependence of arterial smooth muscle tone. *Am J Physiol.* 1990; 259(Pt. 1):C3–C18. [PubMed: 2164782]
2. Lee US, Cui J. BK channel activation: Structural and functional insights. *Trends Neurosci.* 2010; 33:415–423. [PubMed: 20663573]
3. Cui J, Yang H, Lee US. Molecular mechanisms of BK channel activation. *Cell Mol Life Sci.* 2009; 66:852–875. [PubMed: 19099186]
4. Jaggar JH, Porter VA, Lederer WJ, Nelson MT. Calcium sparks in smooth muscle. *Am J Physiol.* 2000; 278:C235–C256.

5. Brayden JE, Nelson MT. Regulation of arterial tone by activation of calcium-dependent potassium channels. *Science*. 1992; 256:532–535. [PubMed: 1373909]
6. Lu R, Alioua A, Kumar Y, Eghbali M, Stefani E, Toro L. MaxiK channel partners: Physiological impact. *J Physiol*. 2006; 570:65–72. [PubMed: 16239267]
7. Orio P, Rojas P, Ferreira G, Latorre R. New disguises for an old channel: MaxiK channel  $\beta$ -subunits. *News Physiol Sci*. 2002; 17:156–161. [PubMed: 12136044]
8. Brenner R, Peréz GJ, Bonev AD, Eckman DM, Kosek JC, Wiler SW, Patterson AJ, Nelson MT, Aldrich RW. Vasoregulation by the  $\beta 1$  subunit of the calcium-activated potassium channel. *Nature*. 2000; 407:870–876. [PubMed: 11057658]
9. Carvalho-de-Souza JL, Varanda WA, Tostes RC, Chignalia AZ. BK channels in cardiovascular diseases and aging. *Aging Dis*. 2013; 4:38–49. [PubMed: 23423545]
10. Leo MD, Bulley S, Bannister JP, Kuruvilla KP, Narayanan D, Jaggar JH. Angiotensin II stimulates internalization and degradation of arterial myocyte plasma membrane BK channels to induce vasoconstriction. *Am J Physiol Cell Physiol*. 2015; 309:C392–C402. [PubMed: 26179602]
11. Leo MD, Bannister JP, Narayanan D, Nair A, Grubbs JE, Gabrick KS, Boop FA, Jaggar JH. Dynamic regulation of  $\beta 1$  subunit trafficking controls vascular contractility. *Proc Natl Acad Sci USA*. 2014; 111:2361–2366. [PubMed: 24464482]
12. Knot HJ, Nelson MT. Regulation of arterial diameter and wall  $[Ca^{2+}]$  in cerebral arteries of rat by membrane potential and intravascular pressure. *J Physiol*. 1998; 508(Pt. 1):199–209. [PubMed: 9490839]
13. Gollasch M, Nelson MT. Voltage-dependent  $Ca^{2+}$  channels in arterial smooth muscle cells. *Kidney Blood Press Res*. 1997; 20:355–371. [PubMed: 9453447]
14. Morello F, Perino A, Hirsch E. Phosphoinositide 3-kinase signalling in the vascular system. *Cardiovasc Res*. 2009; 82:261–271. [PubMed: 19038971]
15. Salamanca DA, Khalil RA. Protein kinase C isoforms as specific targets for modulation of vascular smooth muscle function in hypertension. *Biochem Pharmacol*. 2005; 70:1537–1547. [PubMed: 16139252]
16. Kim HR, Appel S, Vetterkind S, Gangopadhyay SS, Morgan KG. Smooth muscle signalling pathways in health and disease. *J Cell Mol Med*. 2008; 12:2165–2180. [PubMed: 19120701]
17. Sakurada S, Takuwa N, Sugimoto N, Wang Y, Seto M, Sasaki Y, Takuwa Y.  $Ca^{2+}$ -dependent activation of Rho and Rho kinase in membrane depolarization-induced and receptor stimulation-induced vascular smooth muscle contraction. *Circ Res*. 2003; 93:548–556. [PubMed: 12919947]
18. Shimokawa H, Sunamura S, Satoh K. RhoA/Rho-kinase in the cardiovascular system. *Circ Res*. 2016; 118:352–366. [PubMed: 26838319]
19. Cox DH, Aldrich RW. Role of the  $\beta 1$  subunit in large-conductance  $Ca^{2+}$ -activated  $K^+$  channel gating energetics. *J Gen Physiol*. 2000; 116:411–432. [PubMed: 10962017]
20. Nelson MT, Quayle JM. Physiological roles and properties of potassium channels in arterial smooth muscle. *Am J Physiol*. 1995; 268(Pt. 1):C799–C822. [PubMed: 7733230]
21. Fukata Y, Amano M, Kaibuchi K. Rho–Rho-kinase pathway in smooth muscle contraction and cytoskeletal reorganization of non-muscle cells. *Trends Pharmacol Sci*. 2001; 22:32–39. [PubMed: 11165670]
22. Pérez GJ, Bonev AD, Nelson MT. Micromolar  $Ca^{2+}$  from sparks activates  $Ca^{2+}$ -sensitive  $K^+$  channels in rat cerebral artery smooth muscle. *Am J Physiol*. 2001; 281:C1769–C1775.
23. ZhuGe R, Fogarty KE, Tuft RA, Walsh JV. Spontaneous transient outward currents arise from microdomains where BK channels are exposed to a mean  $Ca^{2+}$  concentration on the order of 10  $\mu M$  during a  $Ca^{2+}$  spark. *J Gen Physiol*. 2002; 120:15–27. [PubMed: 12084772]
24. Jaggar JH. Intravascular pressure regulates local and global  $Ca^{2+}$  signaling in cerebral artery smooth muscle cells. *Am J Physiol*. 2001; 281:C439–C448.
25. Wu RS, Marx SO. The BK potassium channel in the vascular smooth muscle and kidney:  $\alpha$ - and  $\beta$ -subunits. *Kidney Int*. 2010; 78:963–974. [PubMed: 20861815]
26. Wang Y-W, Ding JP, Xia X-M, Lingle CJ. Consequences of the stoichiometry of *Slo1*  $\alpha$  and auxiliary  $\beta$  subunits on functional properties of large-conductance  $Ca^{2+}$ -activated  $K^+$  channels. *J Neurosci*. 2002; 22:1550–1561. [PubMed: 11880485]

27. Knaus HG, Garcia-Calvo M, Kaczorowski GJ, Garcia ML. Subunit composition of the high conductance calcium-activated potassium channel from smooth muscle, a representative of the mSlo and slowpoke family of potassium channels. *J Biol Chem.* 1994; 269:3921–3924. [PubMed: 7508434]
28. Sweet T-B, Cox DH. Measuring the influence of the BK<sub>Ca</sub>  $\beta$ 1 subunit on Ca<sup>2+</sup> binding to the BK<sub>Ca</sub> channel. *J Gen Physiol.* 2009; 133:139–50. [PubMed: 19139175]
29. Nimigean CM, Magleby KL. The  $\beta$  subunit increases the Ca<sup>2+</sup> sensitivity of large conductance Ca<sup>2+</sup>-activated potassium channels by retaining the gating in the bursting states. *J Gen Physiol.* 1999; 113:425–440. [PubMed: 10051518]
30. Nimigean CM, Magleby KL. Functional coupling of the  $\beta$ 1 subunit to the large conductance Ca<sup>2+</sup>-activated K<sup>+</sup> channel in the absence of Ca<sup>2+</sup>. *J Gen Physiol.* 2000; 115:719–736. [PubMed: 10828246]
31. Evanson KW, Bannister JP, Leo MD, Jaggar JH. LRRC26 is a functional BK channel auxiliary  $\gamma$  subunit in arterial smooth muscle cells. *Circ Res.* 2014; 115:423–431. [PubMed: 24906643]
32. Yan J, Aldrich RW. LRRC26 auxiliary protein allows BK channel activation at resting voltage without calcium. *Nature.* 2010; 466:513–516. [PubMed: 20613726]
33. Hartmann S, Ridley AJ, Lutz S. The function of Rho-associated kinases ROCK1 and ROCK2 in the pathogenesis of cardiovascular disease. *Front Pharmacol.* 2015; 6:276. [PubMed: 26635606]
34. Xue Y, Li A, Wang L, Feng H, Yao X. PPSP: Prediction of PK-specific phosphorylation site with Bayesian decision theory. *BMC Bioinf.* 2006; 7:163.
35. Nelson MT, Cheng H, Rubart M, Santana LF, Bonev AD, Knot HJ, Lederer WJ. Relaxation of arterial smooth muscle by calcium sparks. *Science.* 1995; 270:633–637. [PubMed: 7570021]
36. Bukiya AN, Liu J, Toro L, Dopico AM.  $\beta$ 1 (*KCNMB1*) subunits mediate lithocholate activation of large-conductance Ca<sup>2+</sup>-activated K<sup>+</sup> channels and dilation in small, resistance-size arteries. *Mol Pharmacol.* 2007; 72:359–369. [PubMed: 17468198]
37. Zhao G, Adebisi A, Blaskova E, Xi Q, Jaggar JH. Type 1 inositol 1,4,5-trisphosphate receptors mediate UTP-induced cation currents, Ca<sup>2+</sup> signals, and vasoconstriction in cerebral arteries. *Am J Physiol Cell Physiol.* 2008; 295:C1376–C1384. [PubMed: 18799650]
38. Bannister JP, Bulley S, Narayanan D, Thomas-Gatewood C, Luzny P, Pachau J, Jaggar JH. Transcriptional upregulation of  $\alpha$ 2 $\delta$ -1 elevates arterial smooth muscle cell voltage-dependent Ca<sup>2+</sup> channel surface expression and cerebrovascular constriction in genetic hypertension. *Hypertension.* 2012; 60:1006–1015. [PubMed: 22949532]
39. Henkel AW, Bieger SC. Quantification of proteins dissolved in an electrophoresis sample buffer. *Anal Biochem.* 1994; 223:329–331. [PubMed: 7534050]
40. Zhao G, Neeb ZP, Leo MD, Pachau J, Adebisi A, Ouyang K, Chen J, Jaggar JH. Type 1 IP<sub>3</sub> receptors activate BK<sub>Ca</sub> channels via local molecular coupling in arterial smooth muscle cells. *J Gen Physiol.* 2010; 136:283–291. [PubMed: 20713546]
41. Xia Z, Liu Y. Reliable and global measurement of fluorescence resonance energy transfer using fluorescence microscopes. *Biophys J.* 2001; 81:2395–2402. [PubMed: 11566809]



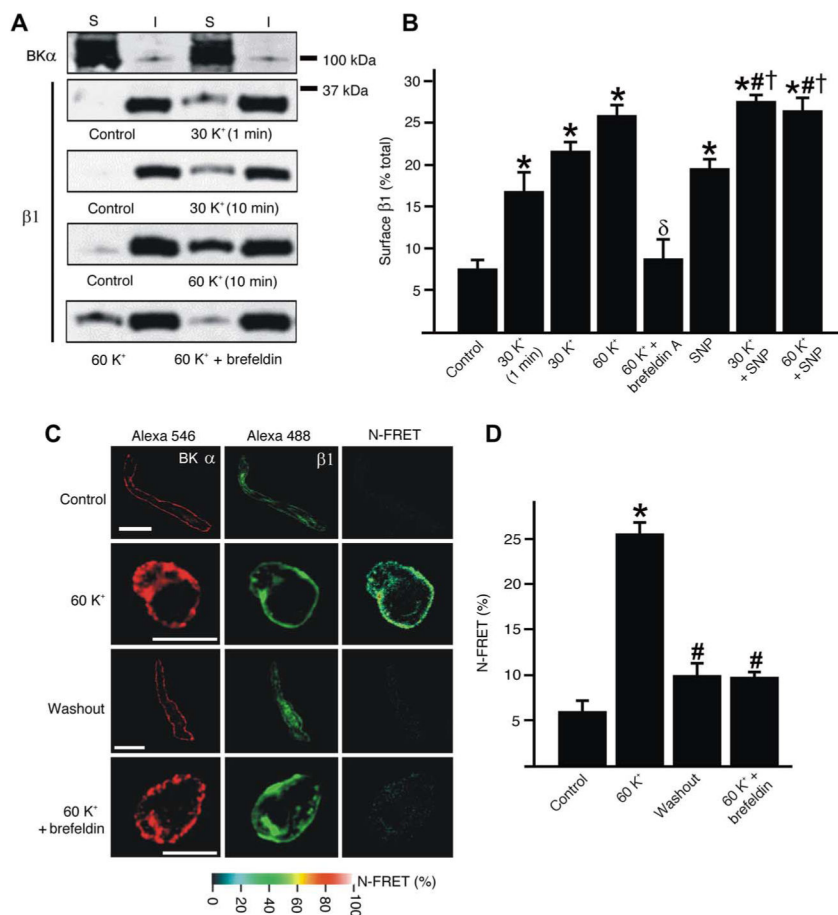


**Fig. 1. Depolarization stimulates surface trafficking of BK β1 subunits in arterial myocytes**  
**(A)** Representative Western blots illustrating surface (S) and intracellular (I) BKα and β1 proteins in rat cerebral arteries obtained using arterial surface biotinylation. **(B)** Mean data,  $n = 6$  to 8 animals for each group; \* $P < 0.05$  compared to control, # $P < 0.05$  compared to SNP, † $P < 0.05$  compared to 30 K<sup>+</sup>, and <sup>δ</sup> $P < 0.05$  compared to 60 K<sup>+</sup> alone. All stimuli were applied for 10 min unless stated otherwise. **(C)** Immunofluorescence images of BKα and β1 and the calculated normalized FRET (N-FRET) under each condition in arterial myocytes. Scale bars, 10 μm. **(D)** Mean data for BKα and β1 immunoFRET,  $n = 6$  images for each group obtained from four different animals; \* $P < 0.05$  compared to control and # $P < 0.05$  compared to 60 K<sup>+</sup>.

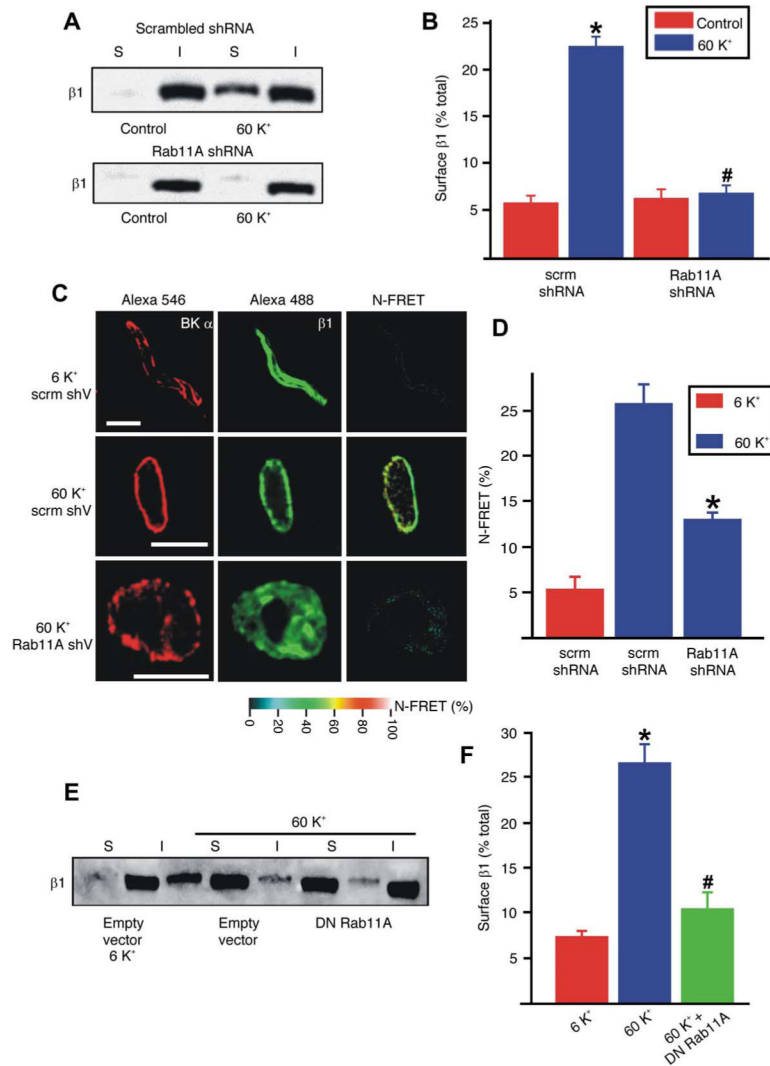


**Fig. 2. Rab11A knockdown inhibits depolarization-induced surface trafficking of  $\beta 1$  subunits in arterial myocytes**

(A) Representative Western blots illustrating surface and intracellular  $\beta 1$  protein in cerebral arteries transfected with scrambled or rab11A shRNA and modulation by 60 K<sup>+</sup> (10 min).

(B) Mean data,  $n = 6$  animals for each group; \* $P < 0.05$  compared to scrambled (scrm) control and # $P < 0.05$  compared to scrambled 60 K<sup>+</sup>.

(C) Immunofluorescence and immunoFRET images of BK $\alpha$  and  $\beta 1$  in arterial myocytes. Scale bars, 10  $\mu$ m.

(D) Mean data,  $n = 6$  images for each group obtained from four different animals; \* $P < 0.05$  compared to scrambled shRNA.

(E) Representative Western blot of  $\beta 1$  protein in depolarized control arteries and arteries expressing dominant-negative (DN) rab11A.

(F) Mean data,  $n = 6$  animals for each group; \* $P < 0.05$  compared to control and # $P < 0.05$  compared to 60 K<sup>+</sup>.

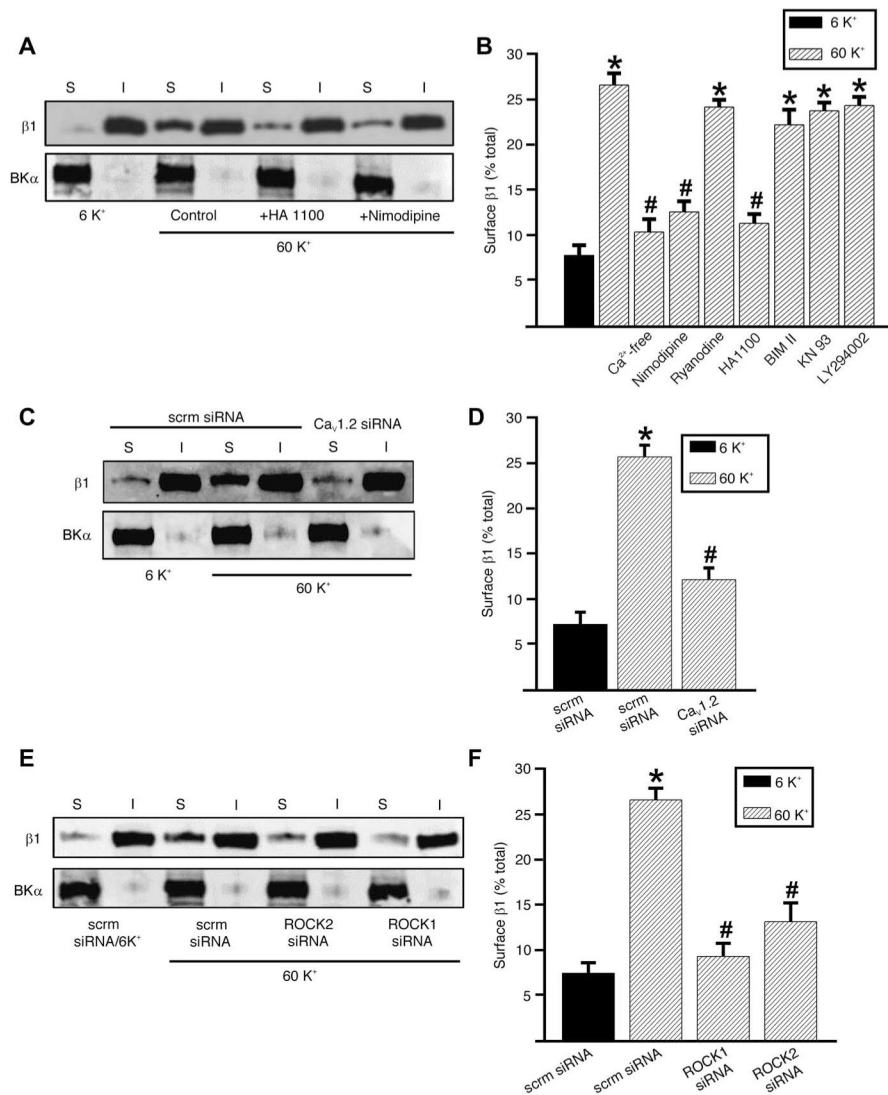


**Fig. 3. Extracellular Ca<sup>2+</sup> removal and Ca<sub>v</sub>1.2 channel and ROCK inhibitors attenuate depolarization-induced  $\beta 1$  surface trafficking in arteries**

(A) Representative Western blots illustrating surface and intracellular BK $\alpha$  and  $\beta 1$  protein using arterial surface biotinylation. (B) Mean data from biotinylation experiments showing effect of extracellular Ca<sup>2+</sup> removal and different antagonists on depolarization-induced changes in the surface abundance of  $\beta 1$  protein,  $n = 6$  animals for each group; \* $P < 0.05$  compared to 6 K<sup>+</sup> and # $P < 0.05$  compared to 60 K<sup>+</sup>. (C) Representative Western blots illustrating surface and intracellular BK $\alpha$  and  $\beta 1$  protein from arteries treated with scrambled siRNA or Ca<sub>v</sub>1.2 siRNA. (D) Mean data,  $n = 5$  animals for each group. (E) Representative Western blots illustrating surface and intracellular BK $\alpha$  and  $\beta 1$  protein from arteries treated with scrambled siRNA or ROCK1 or ROCK2 siRNA. (F) Mean data,  $n = 6$  animals for each group; \* $P < 0.05$  compared to scrambled control and # $P < 0.05$  compared to 60 K<sup>+</sup>.

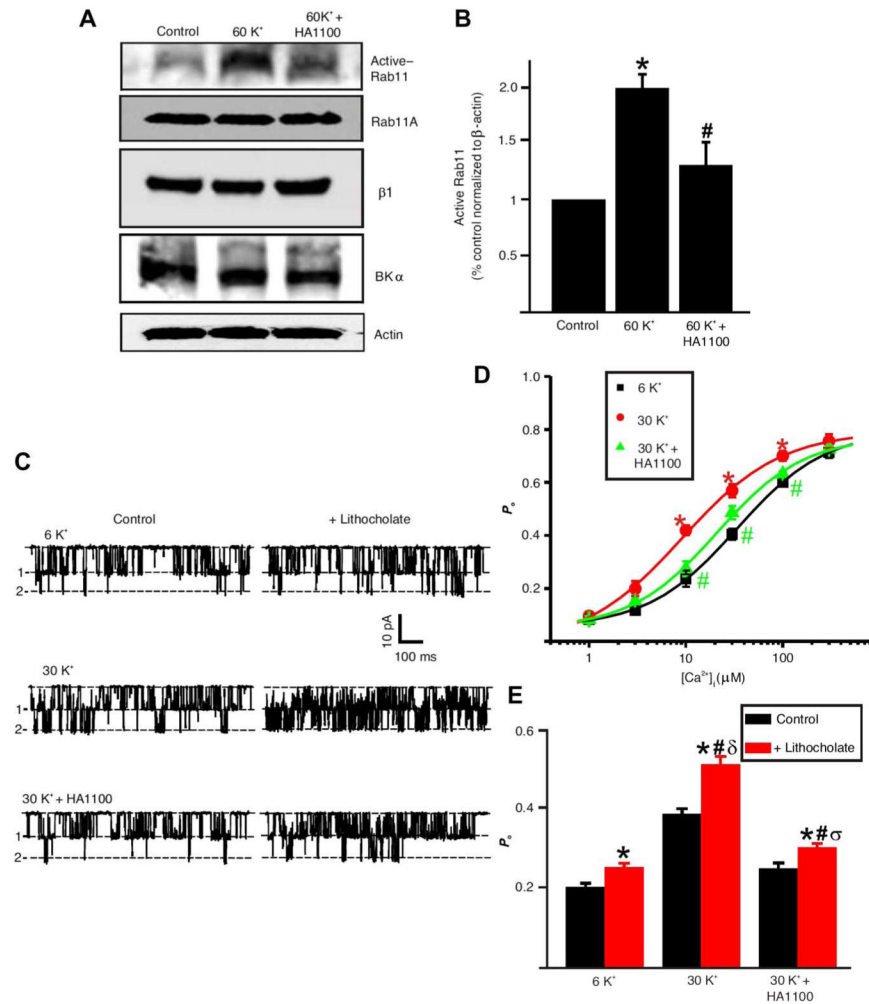


**Fig. 4. Depolarization-induced ROCK activation increases BK channel apparent  $\text{Ca}^{2+}$ -sensitivity in arterial myocytes**

(A) Representative Western blots illustrating total protein from arteries under control conditions, treated with  $60 \text{ K}^+$  or  $60 \text{ K}^+ + \text{HA1100}$  ( $10 \mu\text{M}$ ). (B) Mean data,  $n = 6$  animals for each group;  $*P < 0.05$  compared to control and  $\#P < 0.05$  compared to  $60 \text{ K}^+$ . (C) Representative traces of single BK channel activity and activation by lithocholate in the same patches pulled from either control myocytes ( $6 \text{ K}^+$ ) or myocytes exposed to  $30 \text{ K}^+$  or  $30 \text{ K}^+ + \text{HA1100}$  ( $10 \mu\text{M}$ ). Traces are shown from experiments performed with  $10 \mu\text{M}$  free intracellular  $\text{Ca}^{2+}$  concentration  $[\text{Ca}^{2+}]_i$ . (D) Mean data,  $n = 6$  recordings for each data point;  $*P < 0.05$  compared to  $6 \text{ K}^+$  and  $\#P < 0.05$  compared to  $30 \text{ K}^+$ . (E) Mean data illustrating lithocholate activation of BK channels with  $10 \mu\text{M}$  free  $[\text{Ca}^{2+}]_i$ ,  $n = 6$  recordings for each data set obtained from eight different animals;  $*P < 0.05$  compared to  $6 \text{ K}^+$  control,  $\#P < 0.05$  compared to respective control under the same condition, and  $\delta P < 0.05$  compared to  $30 \text{ K}^+ + \text{lithocholate}$ .

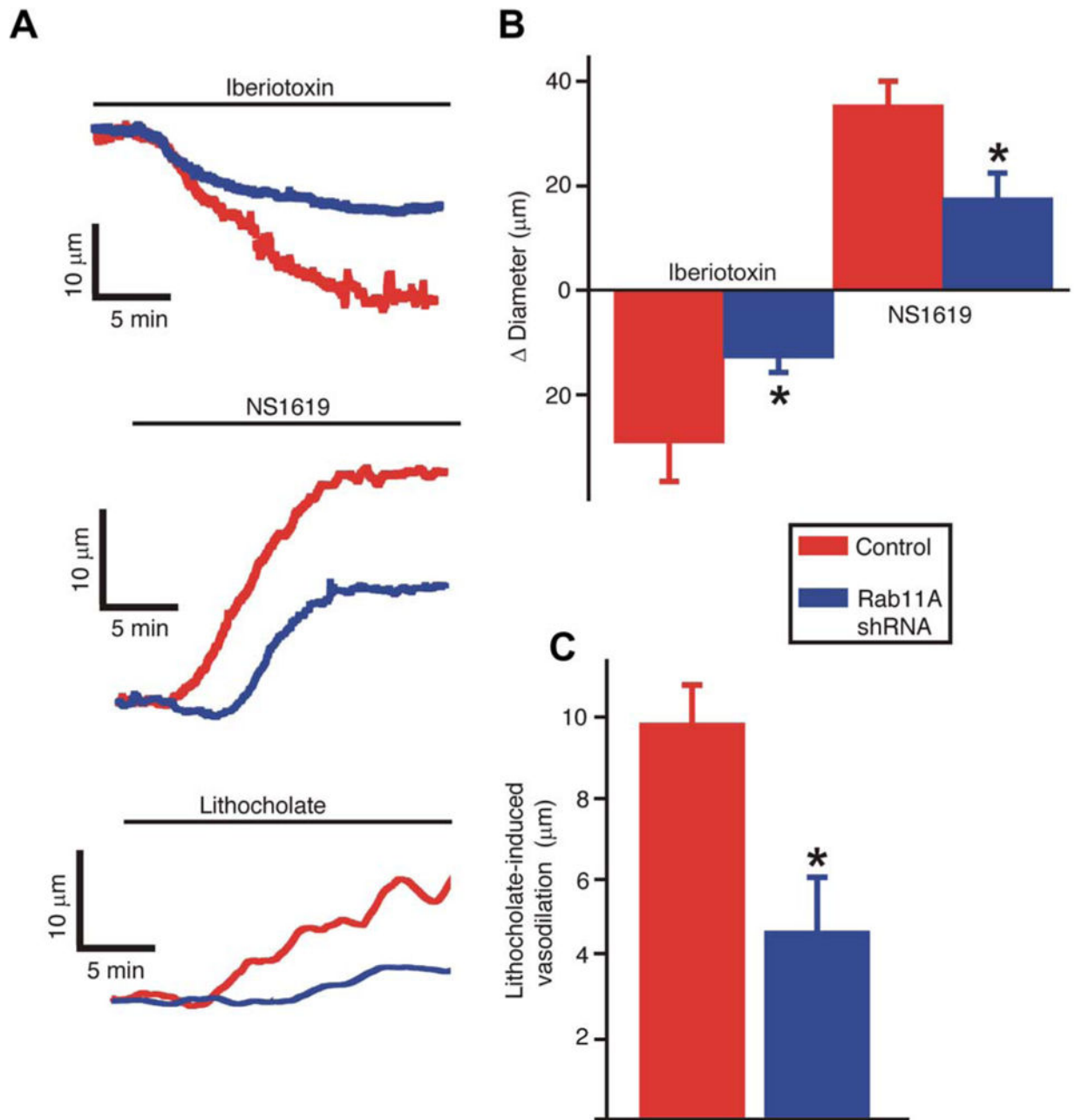


**Fig. 5. Rab11A knockdown inhibits BK channels in pressurized arteries**

(A) Original diameter recordings illustrating constriction in response to iberiotoxin, dilation in response to NS1619, and dilation in response to lithocholate in either control (red trace) or rab11A knockdown (blue trace) arteries. (B) Mean data,  $n = 6$  animals for each group;  $*P < 0.05$  compared to control. (C) Mean data illustrating dilation to lithocholate,  $n = 6$  animals for each group;  $*P < 0.05$  compared to control.